A fractal model for silica aerogels

1994 J. Phys.: Condens. Matter 6 1483

(http://iopscience.iop.org/0953-8984/6/8/007)

J. Phys.: Condens. Matter 6 (1994) 1483–1496. Printed in the UK

A fractal model for silica aerogels

A Rahmani, C Benoit and G Poussigue

Groupe de Dynamique des Phases Condensées URA CNRS 233, Université Montpellier II—Sciences et Techniques du Languedoc, Place Eugène Bataillon, 34095 Montpellier Cédex 5, France

Received 3 August 1993, in final form 8 November 1993

Abstract. We have studied the density of states (DOS) of the fracton regime, which is localized in the very-low-frequency region (less than 1/100 of the spectrum), of a very large (more than 10^6 atoms) realistic model for silica aerogels. Our model is based on a percolating fractal structure, with an homogeneous particle represented by a sample of vitreous silica (v-SiO_2), given by a molecular dynamics simulation. Interactions are represented by the Born–Mayer–Higgins potential. To evaluate the DOS we have developed the linear-frequency moments method, which allows us to compute the DOS of a very large system with great efficiency in the low-frequency region. A comparison with the experimental results for silica aerogels is reported.

1. Introduction

Recently the fractal description has been used intensively to treat the microscopic structure and the dynamics of inhomogeneous systems. Thus, for realistic fractal systems, theoretical work (Alexander and Orbach 1982, Alexander *et al* 1983, Feng and Sen 1984, Grest and Webman 1984, Alexander 1986, Yakubo and Nakayama 1987, 1989) suggests that at intermediate length scales l, between their homogeneous particle size a and their correlation length ξ, the vibrational density of states (DOS) $g(\omega)$ is particularly simple:

$$g(\omega) \simeq \omega^{\tilde{d}-1} \tag{1}$$

where $\tilde{d}$ is the spectral (fracton) dimension. One can recognize weakly localized acoustic phonons at $l > \xi$ and particle modes at $l < a$. In addition to the phonon–fracton ω_ξ and the fracton–particle ω_a crossover frequencies, it is found that for the standard discrete percolating networks model, there exists a new crossover length scale $l_c \simeq 1/\omega_c$ which depends on the relative strength of the microscopic bond-stretching and bond-bending elastic force constants, such that if $l_c > a$, for $l < l_c$, the bond-stretching motion is energetically favourable, whereas for $l > l_c$, the bond-bending motion becomes dominant (Feng 1985). Thus, when ω_c is smaller than ω_ξ, the fracton properties of the system are governed by $\tilde{d} = \frac{4}{3}$, in conformity with the Alexander and Orbach conjecture (1982), whereas when ω_c is much larger than ω_ξ there is an interesting crossover from an effective spectral dimension $\tilde{D}$ to $\tilde{d}$ as the frequency is increased through the fracton regime. $\tilde{D}$ is close to 0.9 (Webman and Grest 1985).

On the other hand, using small-angle neutron scattering (SANS), Courtens *et al* (1987a, b, 1988), Vacher *et al* (1988) and Reichenauer *et al* (1989) showed that porous silica aerogels reveal a fractal structure for a wide range of densities, with fractal dimension $D = 1.8$–2.4.

0953-8984/94/081483+14$19.50

Combining neutron, Raman and Brillouin spectroscopies they identified in the DOS spectrum three crossovers (Vacher *et al* 1990, Bernasconi *et al* 1992), and two distinct regions in the fracton regime of samples of different microstructures that they associated with bend- and stretch-dominating elasticities (Vacher *et al* 1990).

To interpret the dynamical behaviour of these systems, we have studied the dynamical properties of site and bond percolation (Rahmani *et al* 1993). Based on the Born potential with first and second neighbours, our models, where we supposed that each site of the percolating cluster was occupied by a punctual particle, showed that it is difficult to deduce clearly the nature of the contributions of the DOS of silica aerogels. So, the construction of a model based on a more realistic structure and potential energy seems to be necessary.

A primary goal of this work is to build a realistic fractal model that is able to reproduce the different contributions in the DOS of silica aerogels. To do this, it is not only necessary to work on a very large system (more than 10^6 atoms) that is able to generate fracton modes, but one must use computational techniques that are sufficiently powerful to treat these systems.

To specify the numerical method used, we shall in this paper call the method which allows us to determine the squared-frequency distribution function $G(\omega^2)$, the squared-frequency moments method and the method used to compute the DOS $g(\omega)$ the linear-frequency moments method.

The squared-frequency moments method is a powerful tool for the determination of the linear response (infrared, Raman and inelastic neutron scattering) of harmonic systems (Benoit 1987, 1989, Benoit and Poussigue 1989, Benoit *et al* 1990, Poussigue and Benoit 1990, Poussigue *et al* 1991). As is well known, the method is not only simple but can be applied to very large systems, whatever the type of atomic forces, dimension of space or the structure of the material. The method applied to the calculation of the total DOS presents some difficulties at very low frequencies. Nevertheless, the DOS of very large percolating clusters (up to 10^6 atoms) has been computed (Benoit *et al* 1992a, b, Royer *et al* 1992, Rahmani *et al* 1993). Indeed, the method seems to be very efficient in the analysis of spectra between u_{max} and 10^4 ($u_{max} = \omega_{max}^2$; ω_{max} is the maximal frequency of the spectra).

Experimental data concerning silica aerogels show that the fracton region is localized at frequencies less than 300 GHz, whereas $\omega_{max} \sim 36\,000$ GHz. So, at the very outset, we cannot apply the squared-frequency moments method to the study of the fracton region of a realistic system. To do this, we have developed a particularly new and productive form of the moments method: the linear-frequency moments method, which allows us to reach the frequency region below $u_{max}/10^4$, by providing directly the total DOS $g(\omega)$. In fact, by using the squared-frequency moments method, one computes first the function $G(u)$, where $u = \omega^2$, and from there one deduces the function $g(\omega)$, thanks to the relation

$$g(\omega) = 2\omega G(\omega^2)$$

where $g(\omega)\,d\omega$ is the fraction of frequencies in the interval $(\omega, \omega + d\omega)$.

In the following, we present a numerical computation of the DOS using the linear-frequency moments method, which allows a direct determination of $g(\omega)$.

2. Computational procedure

As we mentioned above, thanks to the squared-frequency moments method, we can calculate the function $G(u)$ which is given by

$$G(u) = \sum_j \delta(u - \omega_j^2) = \sum_j \delta(u - \lambda_j) \tag{2}$$

where $\lambda_j = \omega_j^2$ is the jth eigenvalue of the dynamical matrix $\mathbf{D}$ of the system. To calculate the DOS function $g(\omega)$:

$$g(\omega) = \sum_j \delta(\omega - \omega_j) \tag{3}$$

where $\omega_j = \sqrt{\lambda_j}$, we take the $2N \times 2N$ matrix Φ (N is the size of $\mathbf{D}$) defined by

$$\Phi = \begin{pmatrix} \mathbf{0} & \mathbf{I} \\ \mathbf{D} & \mathbf{0} \end{pmatrix}$$

where $\mathbf{I}$ is the $N \times N$ identity matrix. It is easy to show that the eigenvalues of Φ are $\pm\omega_j$.

If the squared-frequency moments method is based on the matrix $\mathbf{D}$, the frequency moments method is based on the matrix Φ. From definition (3) $g(\omega)$ can be written as

$$g(\omega) = -(1/\pi)\mathrm{Im}_{\varepsilon \to 0^+}[\mathcal{R}(z)] \qquad \text{with } z = \omega + \mathrm{i}\varepsilon \tag{4a}$$

where $\mathcal{R}(z)$, the Stieltjes transform of $g(\omega)$, is given by

$$\mathcal{R}(z) = \mathrm{Tr}[(z\mathbf{I} - \Phi)^{-1}]. \tag{4b}$$

At this stage, one can see that the frequency moments method follows the same procedure as the squared-frequency moments method. Thus, $\mathcal{R}(z)$ is then obtained by (Benoit *et al* 1992b)

$$\mathcal{R}(z) = (1/AM)\sum_{\alpha=1}^{M} \mathcal{R}^{\alpha}(z) \tag{4c}$$

where

$$\mathcal{R}^{\alpha}(z) = \langle q^{\alpha} | (z\mathbf{I} - \Phi)^{-1} | q^{\alpha} \rangle \tag{4d}$$

where $|q^{\alpha}\rangle$ is a vector whose components are randomly and uniformly distributed between 0.5 and -0.5, α is an integer varying from 1 to M ($M \to \infty$), A is a normalization constant equal to $\frac{1}{12}$, and for any α and β there is the relation

$$(1/2N)\langle q^{\alpha} \mid q^{\beta} \rangle = A\delta_{\alpha\beta}.$$

With the conditions that Φ is large enough and homogeneous, it is sufficient to take M equal to one (or a small number). In our calculations we take $M = 1$.

The method now consists of expanding $\mathcal{R}^{\alpha}(z)$ in a continued-fraction expansion (Stieltjes 1884, Gaspard and Cyrot-Lackmann 1973, Jurczek 1985):

$$\mathcal{R}^{\alpha}(z) = \cfrac{1}{z - a^{\alpha}_1 - \cfrac{b^{\alpha}_1}{z - a^{\alpha}_2 - \cfrac{b^{\alpha}_2}{z - a^{\alpha}_3 - \cdots \cfrac{b^{\alpha}_n}{z - a^{\alpha}_n - \phi(z)}}}} \tag{5}$$

where $\phi(z)$ is the infinite tail of the fraction. The coefficients a_s^α and b_s^α are derived from Φ and are given by

$$a_{s+1}^\alpha = \tilde{\nu}_s^\alpha / \nu_s^\alpha \qquad \text{and} \qquad b_s^\alpha = \nu_s^\alpha / \nu_{s-1}^\alpha \tag{6}$$

where ν_s^α and $\tilde{\nu}_s^\alpha$ are the spectral generalized moments defined by (Benoit 1987)

$$\nu_s^\alpha = \langle q^\alpha | P_s^\alpha(\Phi) P_s^\alpha(\Phi) | q^\alpha \rangle \tag{7a}$$

$$\tilde{\nu}_s^\alpha = \langle q^\alpha | P_s^\alpha(\Phi) \Phi P_s^\alpha(\Phi) | q^\alpha \rangle. \tag{7b}$$

It is easier to show that $\tilde{\nu}_s^\alpha$ equals zero, and consequently a_s^α also. The polynomials $P_s^\alpha(\Phi)$ obey the following recurrence law:

$$P_{s+1}^\alpha(\Phi) = \Phi P_s^\alpha(\Phi) - b_s^\alpha P_{s-1}^\alpha(\Phi) \tag{8}$$

with $P_{-1}^\alpha(\Phi) = 0$ and $P_0^\alpha(\Phi) = 1$.

The determination of the tail $\phi(z)$ is not trivial. Indeed, as shown in Benoit *et al* (1992b), a sharp truncation of the fraction causes the appearance of sharp lines in the calculated spectrum. To obtain a good solution, one analyses the Fourier components of the coefficients b_s. If they exhibit oscillations with the period m ($m > 1$): $b_s^\alpha = b_{s+m}^\alpha$, then the tail will be given by

$$\phi_{s,m}(z) = \frac{Q_{m-2}^\alpha(z) + P_m^\alpha(z) + \sqrt{(Q_{m-2}^\alpha(z) + P_m^\alpha(z))^2 - 4Q_{m-1}^\alpha(z) P_{m-1}^\alpha(z)}}{2P_{m-1}^\alpha(z)} \tag{9}$$

$P_s^\alpha(z)$ obeys the recurrence law (8) and $Q_s^\alpha(z)$ obeys the following:

$$Q_{s+1}^\alpha(z) = zQ_s^\alpha(z) - b_s^\alpha Q_{s-1}^\alpha(z)$$

with $Q_{-1}^\alpha(z) = 0$, $Q_0^\alpha(z) = 1$.

As we shall see, a very good agreement is noted between the frequency and the squared-frequency moments method. However, calculations show that a greater number of moments are required with the second method (more than 400). In the case of the first method, about 200 moments are sufficient.

3. Physical model

Our realistic fractal model for silica aerogels is based on a 3D infinite cluster percolation structure (figure 1). The homogeneous particle of our aggregates is a 96-atoms (32 silicons and 64 oxygens) sample of vitreous silica (v-SiO_2), with a base size of 10 Å in X and Y, and 14 Å in Z, given by a molecular dynamics simulation (Garofalini 1982, Garofalini and Levine 1985, Feuston and Garofalini 1988).

The potential used in this study is given by the modified Born–Mayer–Higgins equation, which has been used as the effective potential in the molecular dynamics simulation (Garofalini 1982). This potential has been shown to be a good potential to reproduce the experimentally determined radial distribution function, bond-angle distribution and

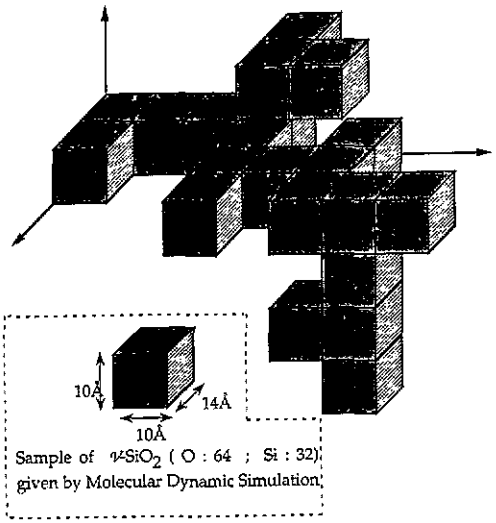

Figure 1. A schematic diagram of the model for silica aerogels: samples are placed on sites of an infinite 3D percolating cluster.

frequency spectrum for bulk silica and silicate glasses. This equation gives the potential between atoms i and j as

$$V_{ij}(r_{ij}) = A_{ij}\exp(-r_{ij}/\rho_{ij}) + (Z_i Z_j e^2/r_{ij})\mathrm{erfc}(r_{ij}/\beta_{ij}) \tag{10}$$

where A_{ij} is a short-range repulsive parameter based on ion sizes:

$$A_{ij} = (1 + Z_i/n_i + Z_j/n_j)b_{ij}\exp(\sigma_i + \sigma_j/\rho_{ij})$$

with Z the electronic charge, n the number of valence shell electrons, σ the atomic size (the repulsive radius parameter), r_{ij} the distance between atoms i and j, ρ, β and b adjustable constants, and the function erfc in the Coulomb term is the complementary error function defined by

$$\mathrm{erfc}(r/\beta) = 1 - \frac{2r}{\sqrt{\pi}}\int_0^{1/\beta}\exp(-r^2s^2)\,\mathrm{d}s.$$

The values for ρ, β, and b were determined by analysing the frequency spectrum (DOS) of the isolated homogeneous particle, with a nearest-neighbour cut-off for all interactions equal to 4 Å, using the usual dynamics matrix diagonalization. The isolated homogeneous particle is the sample of v-SiO_2 given by the molecular dynamics simulation, where we exclude periodic conditions in the dynamical matrix calculations. As one can expect, the suppression of these conditions induces instability of the system by the occurrence of negative frequency squares. With the values for A_{ij}, β_{ij} and ρ_{ij} given in table 1, our system is stable and the general features of the spectrum appear to be consistent with experimental data for vitreous silica. The peak in the low-frequency region ($\sim$ 100 cm^{-1}) is related to the shortness of the particle size (figure 2).

Table 1. The parameters used in the Born–Mayer–Higgins potential.

i	j	Z_i	Z_i	A_{ij} (10^{-9} erg)	β_{ij} (10^{-9} erg)	σ_{ij} (10^{-9} erg)	ρ_{ij} (10^{-9} erg)
Si	Si	+4	+4	0.3963	2.2100	1.148	0.5075
Si	O	+4	−2	0.5104	1.2750	1.284	0.5075
O	O	−2	−2	0.1014	2.1510	1.421	0.5075

In our model (Rahmani 1993), we assume that particles are placed at sites of the 3D infinite percolation cluster formed on a regular cubic lattice, with an occupation probability $p \geqslant p_c$ ($p_c = 0.311$), p_c being the percolation threshold.

If $u_\alpha \begin{pmatrix} l \\ i \end{pmatrix}$ denotes the displacement of the atom i of a particle l in the α direction, the set of equations of motion for the atom i is given by

$$m_i \ddot{u}_\alpha \begin{pmatrix} l \\ i \end{pmatrix} = -\sum_{l',\beta,j} \Phi_{\alpha\beta} \begin{pmatrix} ll' \\ ij \end{pmatrix} u_\beta \begin{pmatrix} l' \\ j \end{pmatrix} \qquad (\alpha = 1, 2 \text{ and } 3) \tag{11}$$

with

$$\Phi_{\alpha\beta} \begin{pmatrix} l \\ ii \end{pmatrix} = -\sum_{l',j}{}' \Phi_{\alpha\beta} \begin{pmatrix} ll' \\ ij \end{pmatrix} \tag{12}$$

where $\Phi_{\alpha\beta} \begin{pmatrix} ll' \\ ij \end{pmatrix}$ are the force constants between atoms i and j given by

$$\Phi_{\alpha\beta} \begin{pmatrix} ll' \\ ij \end{pmatrix} = \left[\frac{r_\alpha r_\beta}{r^2} \left(\frac{1}{r} \frac{\partial V_{ij}}{\partial r} - \frac{\partial^2 V_{ij}}{\partial r^2} \right) - \delta_{\alpha\beta} \frac{1}{r} \frac{\partial V_{ij}}{\partial r} \right]_{r=|r_i^0(l) - r_j^0(l')|}. \tag{13}$$

m_i, $r_{i(l)}^0$ are respectively the mass ($m_O = 16$ g/$\mathcal{N}$ and $m_{Si} = 28$ g/$\mathcal{N}$; $\mathcal{N}$ being the Avogadro number) and the equilibrium position of the ith atom (given by the dynamics molecular simulation) in the lth particle. Two particles are called neighbours if the sites that they occupied are first or second neighbours; V_{ij} is the Born–Mayer–Higgins potential (10); its parameters are given in table 1.

4. Results and discussion

To test the accuracy of our technique, we have plotted in figure 2 the DOS of the isolated homogeneous particle obtained by the frequency moments method, the squared-frequency moments method and diagonalization. Excellent agreement is noted between the three methods.

To illustrate the efficiency of the frequency moments method in the very-low-frequency region, we have plotted in figure 3, on a log–log scale, the DOS $g(\omega)$ versus ω of a percolating cluster formed on a cubic lattice of size 65^3 at $p = 0.33$. Interactions are represented by the Born potential (Qiming Li *et al* 1990, Yakubo *et al* 1990, Yakubo and Nakayama 1987, 1989, Webman and Grest 1985):

$$V = \tfrac{1}{2}\alpha \sum_{ij} K_{ij} (\boldsymbol{u}_i - \boldsymbol{u}_j)^2$$

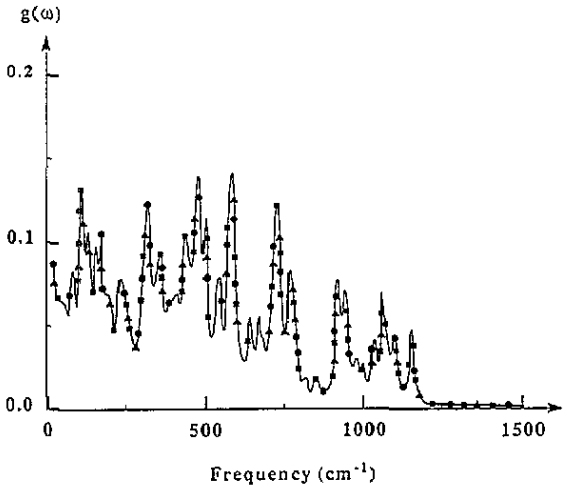

Figure 2. The DOS $g(\omega)$ versus ω for the isolated homogeneous particle (96 atoms), and a test of the linear-frequency moments method. —●—, diagonalization; —■—, squared-frequency moments method; —▲—, linear-frequency moments method.

where the summation is performed over the first-nearest neighbouring pairs (i, j) and u_i is the displacement of the atom i, k_{ij} is a random variable which takes the value 1 if the sites i and j are both occupied, and 0 otherwise, and $\alpha = 0.125$ is the strength of the elastic interaction parameter. The system is represented by an infinite cluster where each site is occupied by a particle of mass $m = 1$. The slope in the fracton region is 0.33 ± 0.02, i.e. the spectral dimension is $\tilde{d} = 1.33 \pm 0.02$, in good agreement with the Alexander and Orbach conjecture ($\tilde{d} = \frac{4}{3}$). One can show also that the frequency moments method has allowed us to reach the low-frequency region down to $\sim \omega_{max}/10^3$, whereas the squared-frequency moments method is limited to $\sim \omega_{max}/10^2$.

To compare the frequency moments method to the squared-frequency method, at very low frequencies in the case of our realistic model for silica aerogels, we have represented, in figure 4, the DOS $g(\omega)$ versus ω, on a log–log scale, of a cluster constructed on a cubic lattice of size 23^3 at $p = 0.33$. One can observe the accuracy of both techniques up to a frequency $\sim$ 400 GHz, which is of the order of $\omega_{max}/100$. Below this frequency the squared-frequency moments method diverges. However, for such a system the lowest frequency must be at least of the order of the lowest-frequency mode of the v-SiO_2 system of size $L = 322$ Å; i.e. $\omega_{min} \simeq 100$ GHz. The frequency moments method seems, with precautions in the computing tail, to reproduce nicely the DOS of the system, as we shall see.

Computations were performed on the same cubic lattice of side $a = 35$, for different occupation probabilities p: (a) $p = 0.321$, (b) $p = 0.325$, (c) $p = 0.331$ and (d) $p = 0.350$. In table 2, we have reported the dimensions x, y, and z, the macroscopic densities ρ and the order N of the dynamical matrix **D** of our aggregate. We have also given the memory occupation and the CPU times necessary to compute one coefficient of the continued fraction for each system.

In figure 5(a), we have reported values for the coefficients b_n versus n for systems (a), (b) and (c). We note a very good stability in the b_n calculation. We observe also that these coefficients exhibit a pseudo-periodicity, which is determined by analysing the b_n Fourier components (figure 5(b)). We note the presence of a pseudo-period close to four. So, to

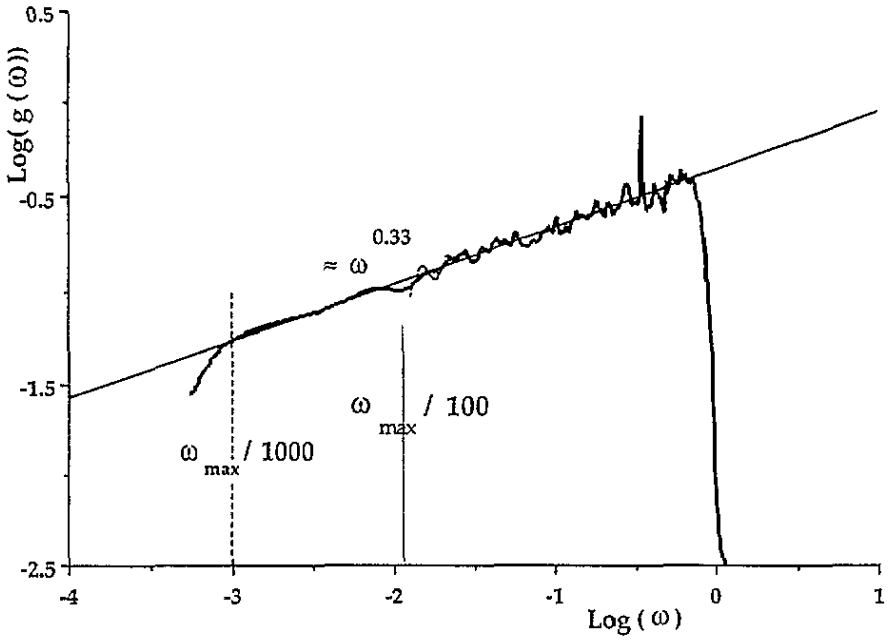

Figure 3. The DOS on a log–log scale for a 3D site-percolating network of size 65^3 at the occupation probability $p = 0.33$ ($p_c = 0.3112$), in the case of the scalar model using the squared-frequency and the linear-frequency moments methods. ——, squared-frequency moments method; ——, linear-frequency moments method.

determine the tail $\phi(z)$ of the continued fraction, and in order to obtain smooth curves, we choose a multiple of four, $m = 16$, in equation (9), which gives more stable results.

In figure 6 we have represented the function $\log(g(\omega))$ versus $\log(\omega)$ for the four systems (a), (b), (c) and (d) defined in table 2. We note that the four curves show a common region above the frequency $\omega_a \sim 300$ GHz. Obviously, this region represents the particle modes. The calculated value for ω_a is in agreement with the experimental value of 250 GHz obtained for the sample designated NH in Vacher *et al* (1990), which is composed of particles of mean size ~ 12 Å (14 Å × 10 Å × 10 Å for our samples) and has a macroscopic density $\rho = 210$ kg m^{-3}.

We observe also in these spectra the presence of an intensive peak near ω_a. In contrast, experimental data show a weak peak in this region. In order to determine the nature of this peak, we have computed the surface projected DOS of our system. To do this, we have taken random charges $|q^\alpha\rangle$ on atoms of the surface which are in a thickness of 2 Å of our aggregate and zero elsewhere. We have reported in figure 7, the surface DOS and the total DOS of a sample formed on a cubic lattice 23^3 at $p = 0.33$. One can show that, qualitatively, the two curves present the same behaviour. The peak observed in the surface DOS is more enhanced than the peak of the total DOS. Hence, one can conclude that the surface modes contribute strongly in the fracton DOS and especially near the crossover ω_a.

The strong intensity of the peak obtained theoretically compared with the experimental intensity can be explained by the structure of our model, which is based on identical homogeneous particles. In real systems, the presence of particles of different sizes could produce a dispersion of the surface modes near ω_a, whereas identical particles could give an accumulation of modes in this region.

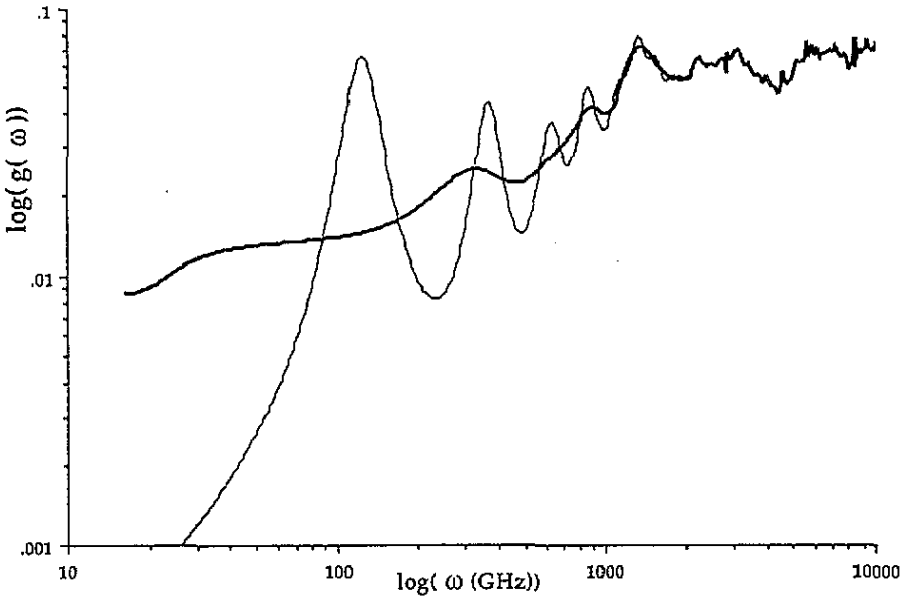

Figure 4. The DOS $g(\omega)$ versus ω, on a log–log scale, for a sample formed on a 3D site-percolating cluster (23^3 cubic lattice at $p = 0.33$) using the squared-frequency and the linear-frequency moments methods. ——, squared-frequency moments method; ——, linear-frequency moments method.

Table 2. Characteristics of the computed aggregates: x, y and z design the dimensions of the aggregates, ρ is the macroscopic density, N is the size of **D** for the four samples (a), (b), (c) and (d); CPU, times necessary to compute one moment; Memory, memory storage required for each system using the linear-frequency moments method.

a	x (Å)	y (Å)	z (Å)	CPU (s)	Memory (Mb)	N	ρ (kg m^{-3})
				11.52	70	537 696	104.8(a)
35	350	350	490	14.31	85	667 872	130.0(b)
				19.60	120	914 976	178.3(c)
				31.54	180	1 472 256	262.3(d)

In regions below ω_a our systems present an accumulation of fractons. Since our model does not include periodic conditions, one does not expect a Debye law in the very-low-frequency region. Nevertheless, it seems that for the dense sample (d) a phonon region begins to set up below ω_ξ.

We remark that the crossover frequency ω_ξ for the weakly dense system (a : $\rho = 105$ kg m^{-3}) is of the order of 10 GHz, whereas $\omega_\xi = 1$ GHz in experiment. This difference can be related to two factors.

(i) The efficiency of the frequency moments method. As established before, the test shows an efficiency of the technique up to $\omega_{max}/1000$, i.e. 35 GHz for silica aerogels. At the very outset, we have no proof that this frequency is the limit of our numerical method. The stability of the obtained result and, as we shall show, the coherent behaviour of the DOS with macroscopic density changes indicate that the linear-frequency moments method is valid at least until 10 GHz.

(ii) This point concerns the structure of our model. We mention, firstly, the choice of

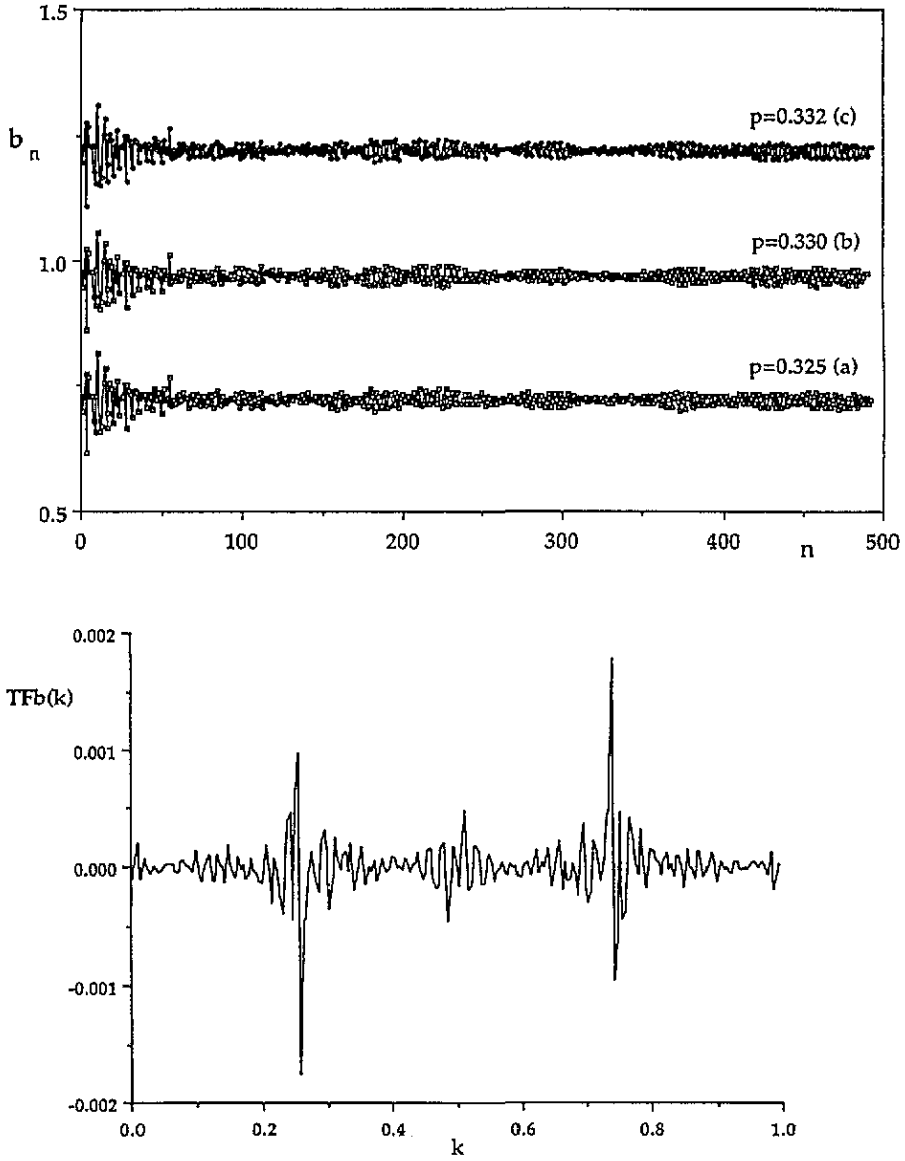

Figure 5. (*a*) Plots of the coefficients b_n versus n for the three systems noted (*a*), (*b*) and (*c*). (*b*) A plot of the Fourier components of the coefficients b_n.

the fractal structure. The percolating model seems to be inadequate for the silica aerogels structure because of its connectivity (Alexander 1989). A soft structure is certainly more representative for that system. If the lowest frequency of our model is smaller than the experimental one, we can deduce that our model is more rigid than silica aerogels. This behaviour can be related to the interaction force intensity. Real systems are composed of particles of different sizes, so the interactions concern a small surface of particles in contact, i.e. weak interactions. In our model, the parallelepiped form of our identical particles reinforces greatly the interactions.

Let us consider the behaviour of the DOS with the macroscopic density (ρ) variations.

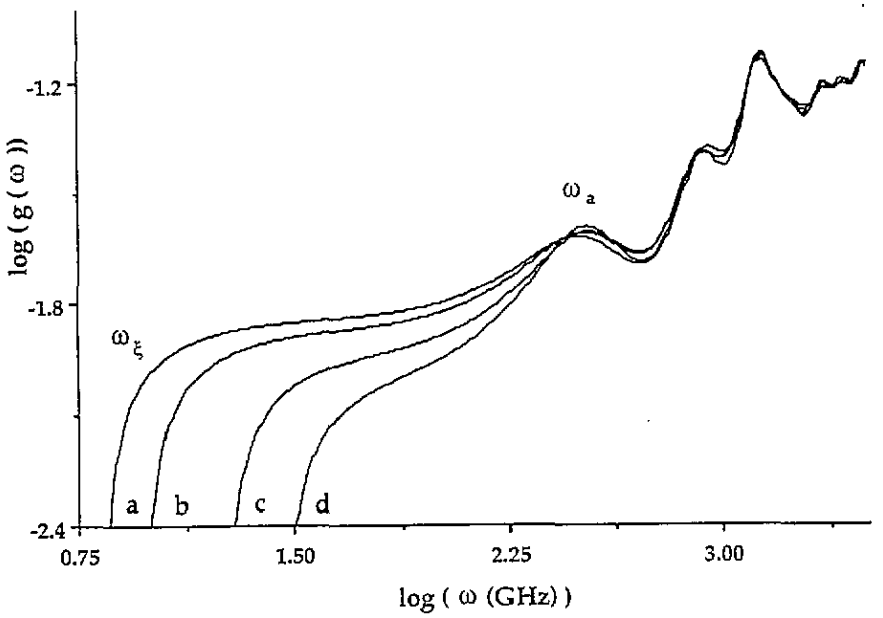

Figure 6. The DOS $g(\omega)$ versus ω, on a log–log scale for the four samples noted (*a*), (*b*), (*c*) and (*d*), which are formed on a 35^3 cubic lattice at values for p of, respectively, 0.3210, 0.3250, 0.3305 and 0.3500.

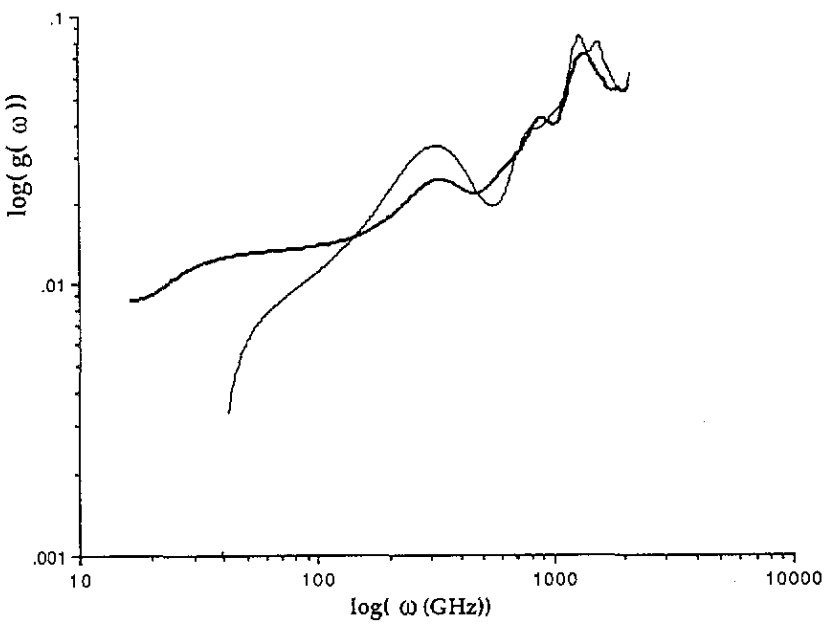

Figure 7. The total and surface DOS $g(\omega)$ versus ω, on a log–log scale, for a sample formed on a 3D site-percolating cluster (23^3 cubic lattice at $p = 0.33$). ——, DOS (surface); ——, DOS (total).

We show that the crossover ω_ξ varies from 10 GHz for the less dense system (a) to 42 GHz for the more dense system (d). This result reproduces the experimental data concerning the increase of the sound velocity with increasing ρ (Conrad *et al* 1989, Courtens *et al* 1987a, b). We have represented, in figure 8, the variations of the frequency ω_ξ versus ρ, on a log–log scale. The slope is equal to 1.54 ± 0.03. Since our model size L is finite, the sound velocity v is given by (Alexander and Orbach 1982)

$$\omega_\xi = 2\pi v(L)/L.$$

We can deduce that

$$v \sim \rho^{1.54 \pm 0.05}.$$

Qualitatively, this behaviour is consistent with results obtained for silica aerogels (Vacher *et al* 1988). This accuracy supports the efficiency of the frequency moments method in determining the low-frequency region of the DOS below $\omega_{max}/100$; $\omega_\xi \sim 10$ GHz for the first system (a).

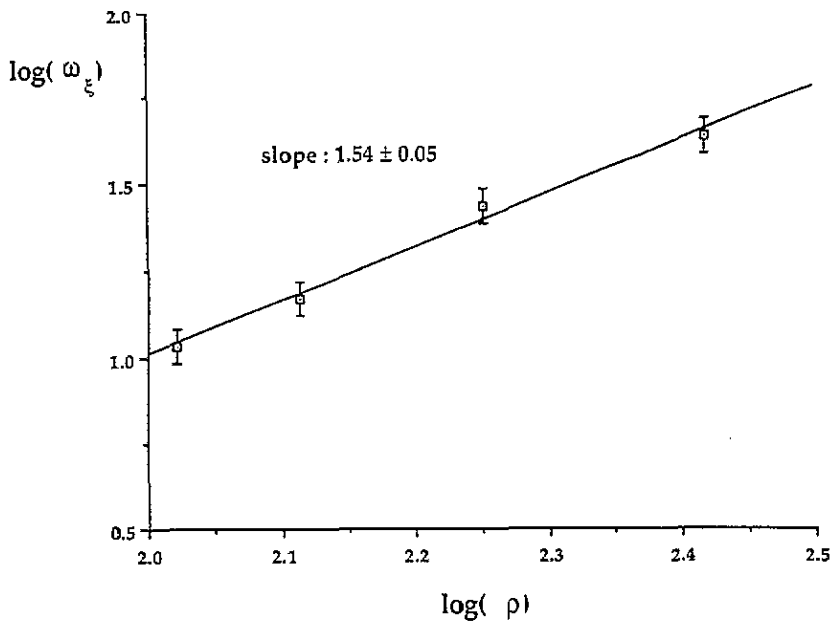

Figure 8. The crossover frequency ω_ξ for the realistic model DOS, versus the macroscopic density ρ, on a log–log scale.

Finally, concerning the two contributions identified in the fracton regime DOS of silica aerogels, which are associated with the stretching and bending elasticities, our model reproduces these contributions. The low-frequency fracton region ($\omega_\xi < \omega < \omega_c \sim 80$ GHz) can be described by an effective spectral dimension $1.00 \pm 0.02 < \tilde{D} < 1.30 \pm 0.02$ for 105 kg m^3 $< \rho <$ 262 kg m^{-3}. It is difficult to analyse the high-frequency fracton region ($\omega_c < \omega < \omega_a$) in terms of an effective spectral dimension because of the presence of

the peak at ω_a. We can conclude that our model reproduces qualitatively the experimental fracton regime of silica aerogels.

In conclusion, we have developed a realistic model for silica aerogels based on infinite percolating clusters, with an homogeneous particle represented by a sample of v-SiO_2 given by a molecular dynamics simulation. Thanks to the frequency moments method, we have calculated the DOS of systems of size ~ 500 Å $\times$ 350 Å $\times$ 350 Å and of different densities. More than 10^6 degrees-of-freedom systems are studied. An excellent efficiency is noted with the frequency moments method in determining the very-low-frequency region below $\omega_{max}/100$. Our model reproduces qualitatively the silica aerogels DOS: particle modes in the *high-frequency region above* $\sim$ *300 GHz followed in the low-frequency region by a fracton* regime sensitive to the macroscopic density. In agreement with reality, we note also that our model shows that the more the macroscopic density increases the more the sound velocity in our systems increases. However, an analysis of the fracton region in terms of effective spectral dimensions is complicated because of the existence of the peak near the frequency ω_a, which is related to the surface modes of our model. It is necessary now to build a model based on another fractal structure, such as diffusion-limited aggregation (DLA), cluster–cluster aggregation (CCA), etc, with a different homogeneous particle of various sizes.

References

Alexander S 1986 *Physica* A **140** 397
—— 1989 *Phys. Rev.* B **40** 7953
Alexander S, Laermens C, Orbach R and Rosenberg H M 1983 *Phys. Rev.* B **28** 4615
Alexander S and Orbach R 1982 *J. Physique Lett.* **43** L625
Benoit C 1987 *J. Phys. C: Solid State Phys.* **20** 765
—— 1989 *J. Phys.: Condens. Matter* **1** 335
Benoit C and Poussigue G 1989 *High Performance Computing* ed J L Delaye and E Gelenbe (Amsterdam: North-Holland) p 347
Benoit C, Poussigue G and Assaf A 1992a *J. Phys.: Condens. Matter* **4** 3153
Benoit C, Poussigue G and Azougarh A 1990 *J. Phys.: Condens. Matter* **2** 2519
Benoit C, Royer E and Poussigue G 1992b *J. Phys.: Condens. Matter* **4** 3125
Bernasconi A,, Sleator T, Posselt D, Kjems J K and Ott H R 1992 *J. Non-Cryst. Solids* **145** 202
Conrad H, Fricke J and Reichenauer G 1989 *Revue Phys. Appl.* **24** C4 157
Courtens E, Pelous J, Phalippou J, Vacher R and Woignier T 1987a *Phys. Rev. Lett.* **58** 128
—— 1987b *J. Non-Cryst. Solids* **95–96** 1175
Courtens E, Vacher R, Pelous J and Woignier T 1988 *Europhys. Lett.* **6** 245
Feng S 1985 *Phys. Rev.* B **32** 5793
Feng S and Sen P N 1984 *Phys. Rev. Lett.* **52** 216
Feuston B P and Garofalini S H 1988 *J. Chem. Phys.* **89** 5818
Garofalini S H 1982 *J. Chem. Phys.* **76** 3189
Garofalini S H and Levine S M 1985 *J. Am. Ceram. Soc.* **68** 376
Gaspard J P and Cyrot-Lackmann F 1973 *J. Phys. C: Solid State Phys.* **6** 3077
Grest G S and Webman I 1984 *J. Physique Lett.* **45** L1155
Jurczek E 1985 *Phys. Rev.* B **32** 4208
Poussigue G and Benoit C 1990 *Phonons 89* (Singapore: World Scientific) p 165
Poussigue G, Benoit C, Sauvajol J-L, Lere-Porte J-P and Chorro C 1991 *J. Phys.: Condens. Matter* **3** 8803
Qiming Li, Soukoulis C M and Grest G S 1990 Phys. Rev. B **41** *11 713*
Rahmani A 1993 *Thèse* Montpellier, France
Rahmani A, Benoit C, Royer E and Poussigue G 1993 *J. Phys.: Condens. Matter* **5** 7941
Reichenauer G, Buchenau U and Fricke J 1989 *Revue Phys. Appl.* **24** C4 145
Royer E, Benoit C and Poussigue G 1992 *J. Phys.: Condens. Matter* **4** 561
Stieltjes T J 1884 *Ann. Ecole Normale* **1** 52
Vacher R, Courtens E, Coddens C, Heidemann A, Tsujimi Y, Pelous J and Foret M 1990 *Phys. Rev.* B **65** 1008

Vacher R, Woignier T, Pelous J and Courtens E 1988 *Phys. Rev.* B **37** 6500
Webman I and Grest G S 1985 *Phys. Rev.* B **31** 1689
Yakubo K, Courtens E and Nakayama T 1990 *Phys. Rev.* B **42** 1078
Yakubo K and Nakayama T 1987 *Phys. Rev.* B **36** 8933
—— 1989 *Phys. Rev.* B **40** 517